14TH CANADIAN MASONRY SYMPOSIUM
MONTREAL, CANADA
MAY 16TH – MAY 20TH, 2021

EVALUATION AND CHARACTERIZATION OF EARLY-AGE MASONRY PROPERTIES

Dunphy, Kyle[1]; Sadhu, Ayan[2] and Banting, Bennett[3]

ABSTRACT

Though masonry is historically one of the world's oldest structural materials, it continues to be implemented in contemporary construction throughout the world. In Canada, loadbearing masonry is comprised of concrete blocks bonded together with mortar. Since a concrete block wall can contain sections of walls that are grouted solid and reinforced as well as portions that are left hollow and unreinforced, masonry is represented as an anisotropic and heterogeneous material with the properties dependent on the directionality of its movement. During the initial construction period, it is established that most masonry structures only exhibit a fraction of their designed strength. The fractional strength is attributed to the active curing of the mortar and grout used in masonry construction during the first 12 to the 24 hours following construction. Current recommendations are that masonry constructed above 1.2 m in height requires some type of bracing against wind loads during these first hours after construction. However, to date, there exist no experimental studies that determine the early-age strength properties of masonry. As such, most wind bracing for masonry construction is designed conservatively, assuming that the masonry will provide no lateral strength. In this study, uniaxial tensile tests are conducted on two-block masonry assemblages with a curing period of 2 to 72 hours to quantify the variation of the elastic properties of the masonry over time. A representative early-age masonry strength is quantified using the experimental data.

KEYWORDS: *masonry structures, construction, experimental testing, stress-strain behaviour, early-age properties*

[1] PhD Student, Department of Civil and Environmental Engineering, Western University, 1151 Richmond Street, London ON, Canada, kdunphy2@uwo.ca
[2] Assistant Professor, Department of Civil and Environmental Engineering, Western University, 1151 Richmond Street, London ON, Canada, asadhu@uwo.ca
[3] Director of Technical Services, Canada Masonry Design Centre, 360 Superior Blvd., Mississauga, ON, Canada, Bbanting@canadamasonrycentre.com

INTRODUCTION

During initial construction periods, masonry walls exhibit only a fraction of the load resistances they are designed for. This fractional strength is attributed to the active curing of the mortar and grout used in masonry construction during the first 12 to the 24-hour period following construction [1]. These 'early-age' masonry structures though having significant strength in the vertical direction due to the self-weight of the components, often have no lateral strength and depend upon a permanent lateral system to provide resistance [1]. Extreme lateral loads induced by earthquakes or wind events have the potential to cause catastrophic failure or damages in these structures, resulting in economic loss or injury to construction works. To mitigate this, external bracing systems have been employed as a temporary lateral system to provide resistance for masonry structures during construction. However, in absence of any standardized procedure, temporary external bracing often results in oversimplifications that contribute to inadequate stability and ultimately premature failure [1-3] of fresh masonry at construction sites. Moreover, to the best knowledge of the authors, no research has been conducted to investigate the behavior of early-age masonry assemblages under 48 hours.

Early research concluded that in most circumstances for masonry structures, the mortar joints act as planes of potential weakness between the blocks. Primarily, this is contributed by the low strength properties of mortar when compared to the block. Moreover, the variability of mechanic bonding between the mortar and block across the interface during curing results in variable bonding strength. As such, significant research has been conducted to quantify the variability of masonry bond strength. Several experimental tests were conducted by [4] to develop a numerical model that quantified the mortar-block interface of concrete masonry assemblages in ABAQUS. Bond wrench tests, diagonal tensions test and shear tests were used to determine the properties of the mortar-block interface under tensile and compressive loading. However, due to the complexity and variance of the experimental results, the authors concluded that developing a generalized robust numerical model for all masonry would be difficult.

An investigation conducted by [5] investigated the material and strength properties of autoclaved aerated concrete (AAC) masonry assemblages. Under tensile loading, the AAC assemblages demonstrated two failure patterns, (1) debonding failure and (2) AAC block failure dependent on the ratio of tensile strength between mortar and masonry. Moreover, the tensile bond stress at failure was better represented using a parabolic stress distribution rather than a linear one. Similarly, a study conducted by [6] investigated the compressive strength of various grouted masonry assemblages with high-strength concrete blocks. Due to the physical process of creating higher strength concrete masonry units, the overall face shells of the block are smoother, resulting in reduced mechanical bonding, therefore, reducing overall bond strength. A novel flexural bond strength test was proposed by [7] based on a z-shaped configured masonry assemblage. Contrasting traditional approach including the bond wrench, brench and direct tensile tests, the proposed method allows for the flexural bond strength parallel to the bed joint to be easily determined from three-point bending. Under tensile loading, it was demonstrated the primary

failure pattern was debonding occurring at a single mortar-brick interface with significantly reduced variation in failure load.

However, the complexities of defining masonry behavior are not limited to the development of accurate constitutive models but the variety of materials that are defined as 'masonry' constituents. As such, many studies have been conducted to quantify the influence of independent material and geometric properties on the strength behaviors of masonry. [8] applied numerical models of microscopic movement of water in cementitious materials available in the literature to evaluate the influence of water flow on block-mortar bond strength. It was concluded that for each block-mortar combination, there is an optimal initial absorption rate (IRA) that results in the maximum bond strength. [9] concluded similarly the IRA had a predominant influence over the compressive strength of clay-brick masonry assemblages.

Recently, research has focused on defining material properties and strength parameters for advanced composite concrete materials for blocks and mortars. The increased bond strengths due to thin, high-strength polymer mortars on the in-plane shear capacity of masonry walls were quantified by [10]. ABAQUS was implemented to create a microscopic 2D model based on shear, and flexural bond capacities as well as compressive strength and modulus of rupture were determined experimentally. The flexural and shear bond strength capacity was demonstrated to be twice that of standard concrete masonry reported in existing standards when using higher strength mortars. The effect of unmortared end web shells on compressive strength for concrete hollow block units with high-strength polymer mortar was quantified by [11]. Testing was conducted autonomously using digital image correlation to determine the deformation of the masonry assemblages during axial compression tests. The addition of polymer in the mortar allowed for better adhesion at the mortar-block interface resulting in higher bond strength when compared to those assemblages using traditional cement mortars.

Though significant research has been conducted to quantify and numerically represent the strength behavior of masonry properties, there currently is no available research regarding early-age masonry properties. This paper attempts to investigate the material behavior of concrete block masonry assemblages during a preliminary curing period of 72 hours. Uniaxial tensile tests were conducted on 98 concrete block assemblages to obtain statistically representative trends of the variation of interface debonding stress and modulus of elasticity with respect to the curing time.

EXPERIMENTAL SETUP

Testing Apparatus

A modified testing apparatus was constructed at Canada Masonry Design Centre (CMDC) to test two-block masonry assemblages under compression and tension. For tensile tests, the apparatus consists of a primary square-shaped steel frame constructed from HSS sections that support two L-shaped brackets connected by steel threaded rods and nuts on either side centerline at the base. These brackets and rods secure the bottom block of the masonry assemblages while testing is being

conducted establishing a fixed base condition. Moreover, the top block is supported by two steel plates that are aligned perpendicular to the face shells of the units. To ensure no slippage occurs between the block and plates during testing, threaded steel rods with a nut on either end run along the length of the block and through each plate thus allowing for the appropriate contact pressure to be established. The plates are connected to a secondary steel frame which is supported by a bottle jack and load cell used for applying and monitoring the load. Figure 1 depicts the configuration of the testing apparatus for uniaxial tensile testing. This novel set-up was decided upon due to concerns about the very weak mortar strengths and their ability to be tested under conventional flexural bond tests such as the bond wrench test. This approach was selected to minimize disturbences to the mortar joint and reduce variability associated with bond wrench tests.

Figure 1: Testing apparatus configuration for tensile testing at CMDC.

Testing Apparatus

The load cell monitors the load applied by the bottle using the software 'OMEGA Digital Transducer Application'. During testing, the load is monitored continuously with the user-defined sampling rates between 1-10 Hz, and individual tests are exportable as .xlxs files. As the load is monitored in pounds, a conversion factor of 4.45 was used to convert the results to Newtons for the purpose of numerical analysis.

For tensile testing, the weight of the second frame and bottle jack must be accounted for as the load cell recorded not only the load applied by the jack but a portion of testing apparatus' weight as well. Moreover, significant tightening of the nuts on the threaded rods had the potential to apply a compressive or tensile load to the sample before the start of the test. A set of 1000 samples were recorded by the load cell and the mean value of those samples was taken as the weight of the frame with no load applied at the start of each testing day. This value was used to normalize the readings

during the tests conducted that day such that the value of the load applied can be determined. Additionally, while the masonry assemblage was being secured by the apparatus, the load was monitored to ensure no additional tensile load was prematurely applied to the sample. As a surcharge load was already applied to all samples during curing, the application of a small compressive load during nut tightening should not have an impact on numerical results.

Displacement Sensors

Linear variable differential transformers (LVDTs) were implemented to quantify the axial displacements of the masonry assemblages under tensile loading as shown in Figure 2. Two LVDTs were placed on opposite parallel faces of the blocks to measure the strain simultaneously such that the average strain during testing could be determined. As the ratio between the strength of the block and mortar is significantly high, it is assumed that the significant portion of the deformation occurs in the mortar rather than the blocks themselves. The strain under uniaxial tensile loads can be quantified by Eq.1:

$$\varepsilon_t = (\delta - \delta_o)/D_m \quad (1)$$

where ε_t is the elastic tensile strain at failure, δ is the displacement of the assemblage at failure in mm, δ_o is the initial displacement of the assemblage at the start of the test and D_m is the depth of the mortar joint; for all samples, this value has been set to 10mm by the mason. To capture the microscopic displacements expected with this elastic deformation, two high-resolution LVDT packages and a wireless data acquisition system (DAQ) were acquired from MicroStrain®. The typical setup of the sensing and acquisition equipment is depicted in Figure 3.

RESULTS

Stress-Strain Behaviors

The displacement and load data collected from the experimental tests were used to develop the stress-strain behavior of the masonry assemblages. During the construction process of the samples, the painter's tape was used to limit the interface bonding area between the mortar and block allowing for a constant cross-sectional area for the determination of the mortar stress to be established. Predominately, it was observed that the failure behavior of the samples under tension was debonding between the block and the mortar at the interface. Figure 4 depicts the typical failure pattern for the masonry assemblages under tensile loads.

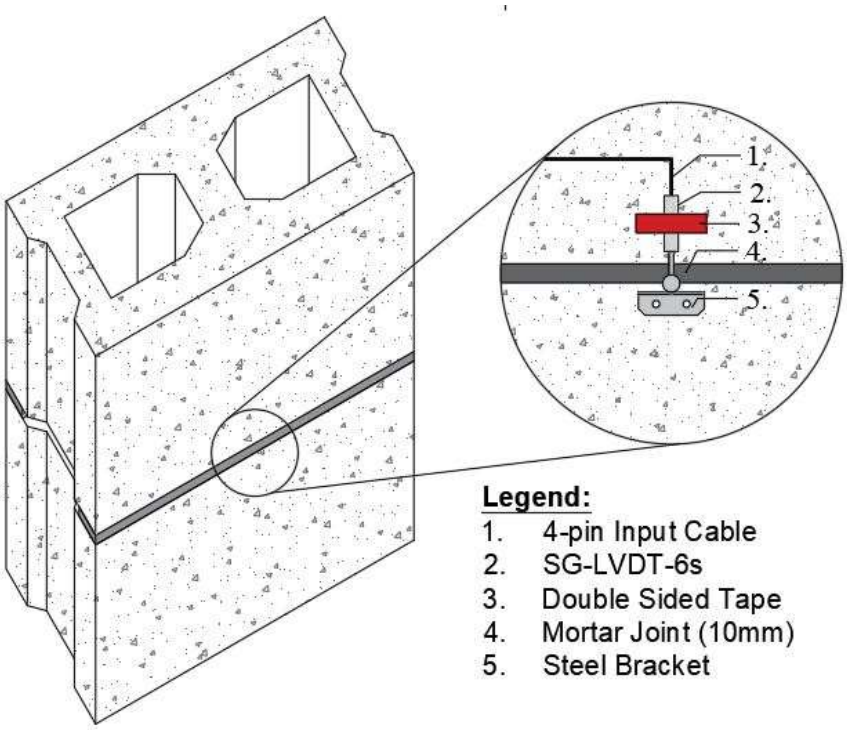

Figure 2: Attachment of LVDTs to masonry specimen.

Figure 3: Displacement sensor and data acquisition set-up.

For each test, the individual time-varying strain data for each sensor was plotted against mortar stress. In addition, the average stress-strain behavior based on the strain data collected from each

sensor was quantified. Linear regression was performed on the average stress-strain, assuming a zero-intercept linear model as represented by Eq. 4 to determine the tensile modulus of elasticity.

$$\sigma = E\varepsilon \tag{4}$$

where σ is the tensile stress in Pa, ε is the tensile strain, and E is the modulus of elasticity in Pa as determined by Eq. 5.

Figure 4: Typical failure pattern of early-age masonry assemblages under tensile loads

$$E = \sum(\sigma\varepsilon)/\sum(\varepsilon^2) \tag{5}$$

where the $\sum(\sigma\varepsilon)$ and $\sum(\varepsilon^2)$ are calculated for each time interval of an individual test. To determine data fit with respect to the linear model, the coefficient of determination (R^2) was determined. However, due to using a zero-intercept model for the linear regression, there is the potential for the R^2 value to be greater than unity as R^2 values increase with this model type. Therefore, an adjustment factor is used to correct for this possibility as represented in Eq. 6.

$$R^2_{adj} = 1 - (1-R^2)((N-1)/(N-k-1)) \tag{6}$$

where R^2_{adj} is the adjusted coefficient of determination, N is the number of the data point in each test sample, k is the number of independent variables, the strain being the independent variable and R^2 is the coefficient of determination as calculated by Eq. 7.

$$R^2 = 1 - (SSE/(SSR + SSE)) \tag{7}$$

where SSE is the sum of the errors between the values predicted by the regression and those determined in the experiment, and SSR is the sum of the residuals between the values predicted by the regression and the mean value of the experimental data. Figures 5 (a-b) show typical stress-strain plots with zero-intercept linear regression models for samples that have undergone 4-hours of curing with varying statistical significance.

Population Statistics

Due to variability of the goodness-of-the-fit of the linear model with the experimental data the overall statistical significance of the sample population is greatly affected. A sample population is considered as a group of samples whose curing time is within +/- 30 minutes of the testing hour. For example, all samples between 3.5 and 4.5 hours of curing time would belong to the 4-hour curing time sample population. As such, two techniques were implemented to improve the statistical significance of the population.

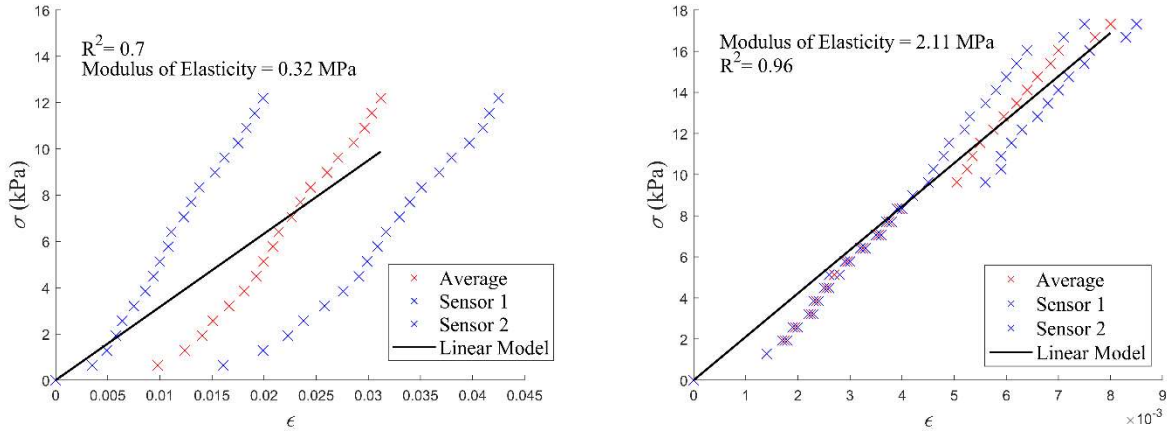

(a) (b)

Figure 5: Stress-strain behavior with (a) low R^2 and (b) high R^2.

Firstly, the effect of excluding those samples whose R^2 values were less than 0.8 and 0.9 was investigated. Secondly, an Extreme Value Analysis (EVA) was performed on the data to exclude samples that had weak and strong outliers in (a) peak stress, (b) peak strain, (c) peak stress and strain and (d) modulus of elasticity. Those values that exceeded 1.5 times the Interquartile Range (IQR) were considered 'Weak Outliers' while those exceeding 3.0*IQR* were considered 'Strong Outliers'. Figure 6 shows a typical EVA analysis of the 4-hour population. It was concluded that removing those samples with $R^2 < 0.8$ was the most effective technique for improving the statistics of the sample population while excluding the least number of samples. Though EVA techniques were effective at improving the population statistics, they caused a significant reduction of population size; in some groups, almost 50% of the population was excluded.

It can be observed that there is a significant amount of variability within each population for both the modulus of elasticity and peak strain values. Factors such as the IRA of the block, the humidity during initial casting and curing of the samples and the overall surface roughness of the block interface with the mortar would cause sample variation within a population. Moreover, as a bottle jack is used, the load is applied manually and therefore, the loading rate is applied nonuniformly; sudden increases in loading rate may cause samples to fail prematurely over others. Lastly, slight eccentricities of the assemblage with respect to the testing apparatus may cause minor flexural

stresses instead of pure axial stress, which may influence the overall failure behavior of the samples.

Variation of Elastic Properties with Curing Time

To establish a relationship between the peak stress and modulus of elasticity of early-age masonry and curing time all enhanced samples as described in Section 3.2 were plotted. Moreover, when the average modulus of elasticity and peak stress is plotted with respect to the curing time of each population, as seen in Figures 6 (a-b) it can be observed that these plots follow a roughly logarithmic trend. The error bars represent the variation of the parameters in both the x and y-axis. A significant variation is observed in the dependent variable (peak stress or modulus of elasticity); however, minimal variation is present with the active curing time.

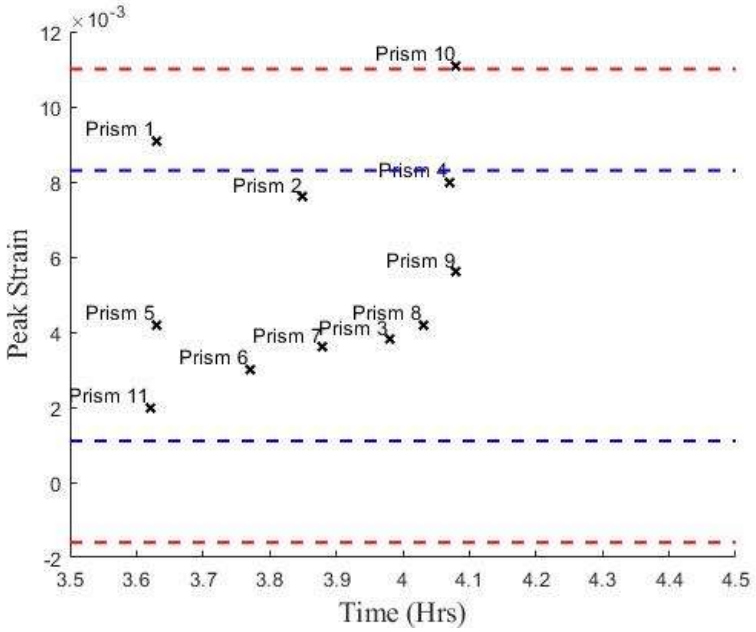

Figure 6: EVA on peak strain for the 4-hour sample population.

Therefore, nonlinear regression was performed on the data present in Figures 7 (a-b), assuming a logarithmic model as depicted in Eqs. 8 and 9.

$$\sigma_f = A*ln(t) + B \quad (8)$$

$$E = A*ln(t) + B \quad (9)$$

Where σ_f is the peak stress at failure and A, B are the nonlinear regression coefficients. However, as seen in Figures 8 (a-b), this trendline only accounts for 50% of the values conservatively and would not be acceptable to use in the design of lateral support systems for early-age masonry.

Therefore, a safety factor, φ, of 0.60, is added to the equation to increase the lower bounds of the equation such that it accounts for a statistically significant portion of the parameters

conservatively. For peak stress, only 3 out of 91 samples fall outside of this confidence interval suggested a statistically reliable correlation. However, even with such a safety factor, there are still many values of modulus of elasticity that fall outside this lower bound; as such more samples should be tested to better establish a time-varying trend for this parameter. Therefore, the proposed Eq. 10 a conservative estimation of the peak stress and modulus of elasticity for early-age masonry structure between 3 – 72 hours of active curing.

$$\sigma = \varphi(A*ln(t) + B) = 7.8ln(t)-1.92 \quad (10)$$

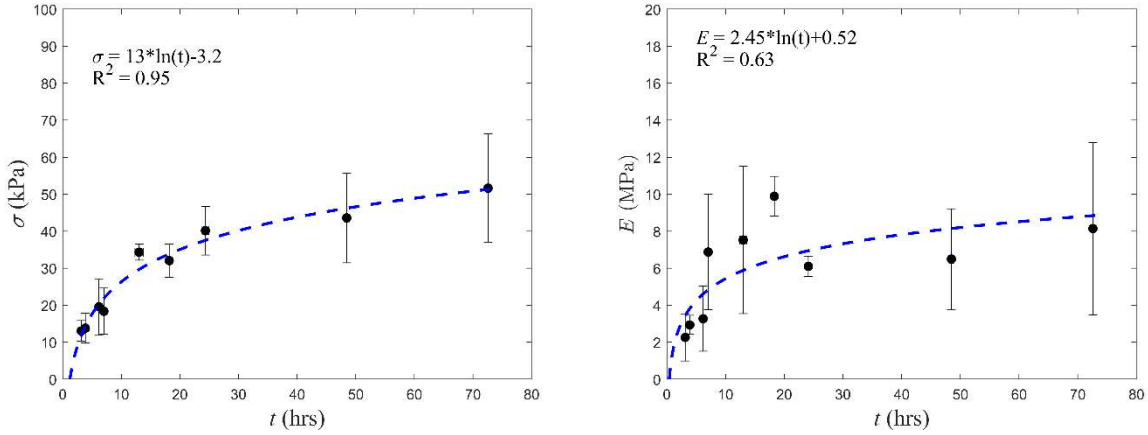

(a) (b)

Figure 7: Nonlinear regression of (a) σ_f and (b) E.

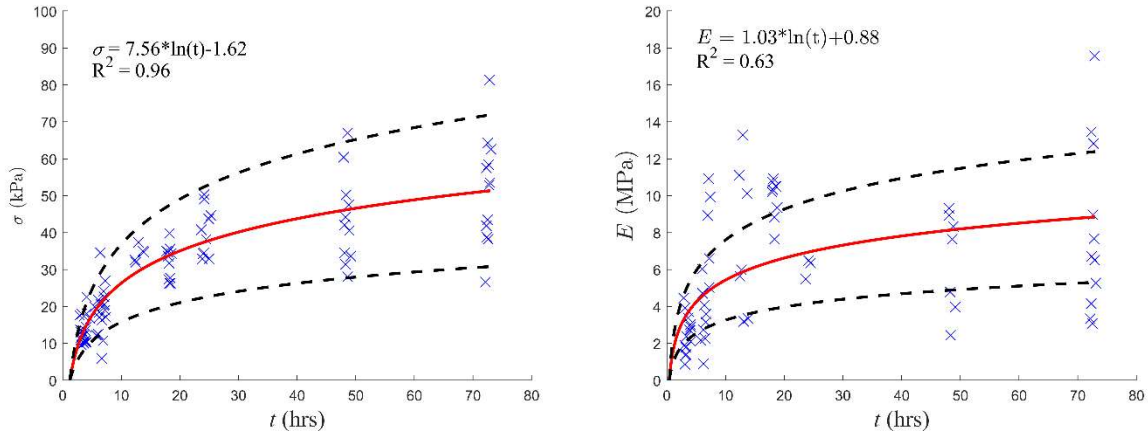

(a) (b)

Figure 8: Boundaries of safety factor for (a) peak stress and (b) E.

CONCLUSIONS

In conclusion, this paper attempted to investigate the material behavior of concrete block masonry assemblages during the preliminary curing period of 72 hours. Numerous masonry assemblages

were constructed and allowed to cure for variable lengths of time and tested under uniaxial tensile loads. From the average stress-strain data, the modulus of elasticity was determined using a zero-intercept linear regression model. Samples within populations exhibiting an $R^2 < 0.8$ were excluded to enhance overall population statistics. Significant variation in stress-strain properties was found due to variation in loading rate, curing humidity, IRA and surface roughness. Finally, a conservative representation of the variation of peak failure stress with respect to curing time was established through nonlinear regression techniques.

ACKNOWLEDGMENT

The authors would like to thank Mitacs and CMDC for providing funding to conduct this research through Accelerate program. The authors would also like to thank the Natural Sciences and Engineering Research Council (NSERC) of Canada for providing financial support through the second author's Alliance grant.

REFERENCE

[1] Walkowicz, S. C. (2013). "Internal Bracing Design Guide for Masonry Walls Under Construction." *International Masonry Institute*. Retrieved on September 7th, 2018 from http://imiweb.org/wp-content/uploads/2015/11/IMIInternalBracingGuide.pdf

[2] Hatzinikolas, R. Z. S. Z. M. (1995). "Temporary Wind Bracing of Masonry Structures." *Canadian Masonry Research Institute*.

[3] Dailey, T. (2018). "The Practical Design of Temporary Masonry Wall Bracing." *SMART Dynamics of Masonry*, 2(3).

[4] Pasquantonio, R. D., Parekian, G. A., Fonseca, F. S. and Shrive, N. G. (2020), "Experimental and numerical characterization of the interface between concrete masonry block and mortar", IBRACON Structures and Materials Journal, 13(3), 578 – 592.

[5] Bhosale, A., Zade, N. P. and Sarkar, P. (2019). "Experimental Investigation of Autoclaved Aerated Concrete Masonry." Journal of Material in Civil Engineering, 31(7).

[6] Fonseca, F. S., Fortes, E. S., Parsekian, G. A. and Camacho, J. S. (2019) "Compressive strength of high-strength concrete masonry grouted prisms." Construction and Building Materials, 202, -861-876.

[7] Khalaf, F. M. (2005), "New Test for Determination of Masonry Tensile Bond Strength", Journal of Materials in Civil Engineering, 17(6), 725 -732.

[8] Groot, C. and Larbi, J. 1999. The influence of water flow (reversal) on bond strength development in young masonry. HERON, 44(2): 63-78.

[9] Kaushik, H. B., Rai, D. C., and Jain, S. K. 2007. Stress-Strain Characteristics of Clay Brick Masonry under Uniaxial Compression. Journal of Materials in Civil Engineering, 19(9): 728-739.

[10] Dhanasekar, M., Thamboo, J. A. and Nazir, S. (2017). "On the in-plane shear response of the high bond strength concrete masonry walls." Materials and Structures, 50(214).

[11] Thamboo, J. A., Dhanasekar, M. and Yan, C. (2013). "Effects of Joint Thickness, Adhesion and Web Shells to the Face Shell Bedded Concrete Masonry Loaded in Compression." Australian Journal of Structural Engineering, 291-302.

[12] Australian Standards (2001). "Masonry Structures." *AS 3700*, Standard Australia International, Sydney, Australia.